Modern trends in selecting and designing Francis turbines

By F. de Siervo* and F. de Leva*

The increasing demand for hydroelectric power has tended to lead to the construction of particularly large units, especially for conditions of low head and high flow. This tendency has stimulated advances in design and manufacturing processes, so as to keep the dimensions and costs of these large units to a minimum without sacrificing efficiency and reliability.

THE USE of increasingly large turbines, which has been brought about by the need to uprate units, as well as to exploit sites more effectively, has been particularly evident in those run-of-river plants where large flows at medium or small heads are utilized. There has been a corresponding incentive to limit the dimensions of these units so as to keep costs both of the mechanical components and the associated civil engineering structures to a minimum; improved efficiency is another factor which is leading to more refined designs.

In the case of Francis turbines the increase of unit size has led to a broadening of the field of application, partially invading those that were once considered exclusive to Kaplan and Pelton machines.

The authors' company has operated for more than twenty years in designing hydropower plants and is currently working on some major projects, from the point of view of unit power and total installed capacity. Experience acquired has made it possible to examine and evaluate advanced manufacturing technology for the solution of the problems concerning the design of hydropower plants.

An accumulation of data, covering in particular the more recent plants, has made it possible to assess current progress in designing Francis turbines, through contacts with manufacturers all over the world and by taking account of modern technology.

The aim of this article is to provide engineers with an up-to-date reference source for preliminary planning at the feasibility study stage. Statistical diagrams of the main dimensional and operating characteristics of Francis turbines are included.

Data analysis

The research detailed in this article covers the period 1960-1975, and takes into account some outstanding vertical shaft Francis turbines built by manufacturers all over the world.

The table gives the main features of the installations investigated as taken from the references, while the diagrams are based on the project data, dimensions, and the general layouts of the machines.

The turbine data presented in the graphs have been collated only from cases with complete information, rejecting those having unusual installation and operating conditions; eg, the data relating to turbines which are coupled to storage pumps or to generators, designed to operate as synchronous condensers without air injection into the runner, were not taken into account in tracing the diagrams of specific speed and cavitation coefficient.

The curves were drawn by a simple regression procedure, using a digital computer program which analyses the interdependence of assigned pairs of values utilizing ten different types of interpolating functions. In the cases examined, the functions which gave the best correlation coefficients were: straight line; exponential; hyperbolic; power; and last, rational.

The values of the correlation coefficients and standard deviations indicated in the text permit, in each case, the evaluation of the degree of association between the two variables under study and of the scattering of the data in respect to the interpolating function.

General selection criteria

Usually the main data available to the engineer when selecting the hydraulic turbine for a preliminrary project or feasibility study, are: net design head, H_n; and design capacity for the turbine, P_t.

Generally these result from complex considerations strictly correlated with the regulation of the catchment

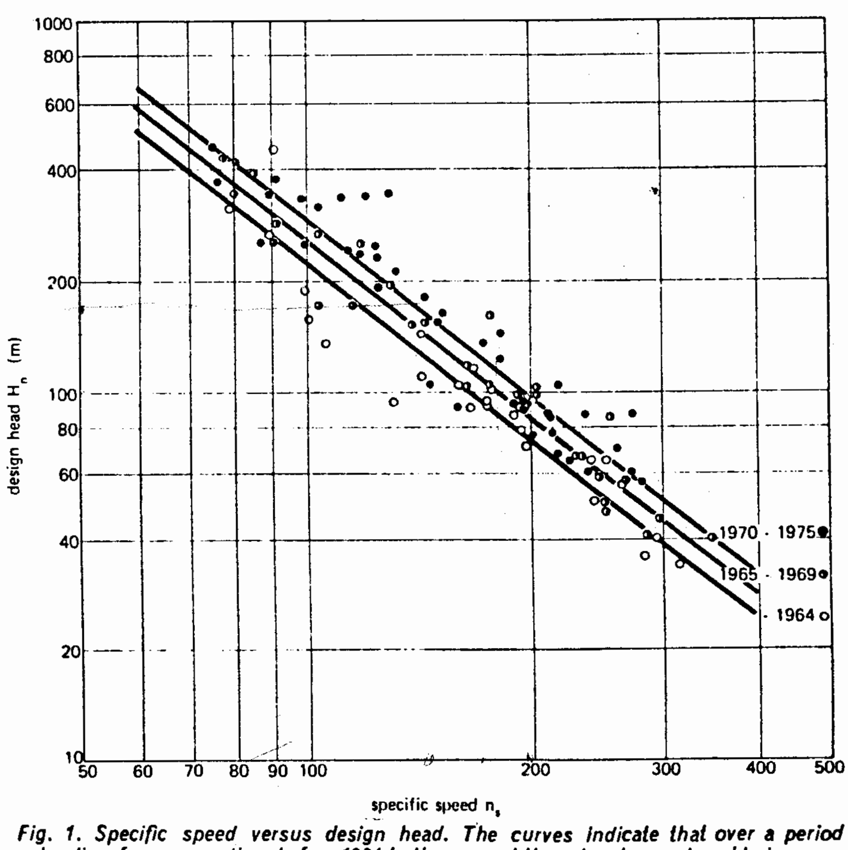

Fig. 1. Specific speed versus design head. The curves indicate that over a period extending from some time before 1964 to the present there has been a trend to increase the value of the specific speed for a given head.

* ELC-Electroconsult, via Chiabrera 8, Milan 20151, Italy.

asin to be utilized, and the requirements of the electric grid to which the powerplant will be connected. The first requirement for the engineer is to choose the most suitable type of turbine for the project under study.

Each turbine is characterized by a constant, called the specific speed:

$$n_s = nP_t^{0.5}H_n^{-1.25} \quad \dots \quad (1)$$

n being the rated speed.

Eq. (1) means that, for all turbines which are geometrically similar and operate in similar hydraulic conditions, and for which the efficiencies are assumed to be equal, the product

$$nP_t^{0.5}H_n^{-1.25}$$

is constant.

Practical experience shows that technical and economical requirements together with manufacturing problems, establish a relationship between the specific speed and the design head, of the type:

$$n_s = F[H_n]$$

which is normally expressed in the form of a diagram. For any assigned value of the head H_n, there exists a restricted range of possible values for n_s, thus determining the type of turbine to be employed.

The available data have been divided into three groups, depending on the year of design of the turbines. This gives the three regression curves indicated in Fig. 1, which are described as follows:

1960–1964	$n_s = 2959.H_n^{-0.625}$
1965–1969	$n_s = 3250.H_n^{-0.625}$
1970–1975	$n_s = 3470.H_n^{-0.625}$

The correlation coefficients and the standard deviations are (respectively):

$r = -0.94$	$s = 52.6$
$r = -0.97$	$s = 30.2$
$r = -0.95$	$s = 39.8$

They show a high degree of grouping of the data in respect of the chosen interpolating functions.

The diagram shows that, over the period considered, there has been a constant trend to increase the value of n_s for a given head. For constant head and design capacity, an increase of the specific speed corresponds to a higher turbine frequency of rotation as in Eq. (1); the increase of n_s thus leads to a reduction in the unit dimensions, and consequently to lower installation costs, while keeping the unit costs for raw materials and labour unchanged.

The curves drawn, give the specific speed for any assigned head and represent an average of the data examined, and therefore serve only to give an indicative value. Single installations may have n_s values that differ from those given by the equations, depending on particular operating or design criteria. For example, the tendency to increase the n_s value will be more apparent in the case of units which are going to be used for peak service where the greater wear problems are compensated by shorter periods of operation; or for larger units, for which the increase of the specific speed permits cost reductions, which are greater in absolute value than in the case of smaller units.

Particularly favourable installation conditions, such as those sometimes encountered in the case of underground powerplants, lead to similar consequences.

The increase in n_s will be less appreciable for units of smaller dimensions where the lower costs do not justify expensive research work, or in the case of improvement or expansion of older powerplants where the installation conditions cannot be altered.

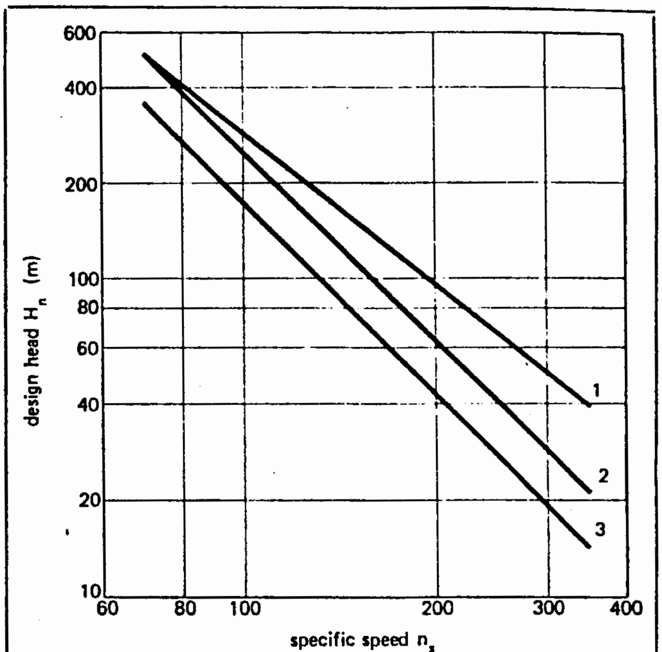

Fig. 2. Increase in specific speed (for a given head) as a function of the period of design. The relationship denoted by (1) is derived from Fig. 1; curve number 2 is derived from Handbook of Applied Hydraulics *published in 1969 and written by Sorensen, K. E. and C. V. Davis; curve number 3 is derived from the US Bureau of Reclamation's* Selecting Hydraulic Reaction Turbines *published in 1966.*

The general trend over the years towards higher specific speeds for given heads is confirmed by Fig. 2.

Once the value of n_s is decided from Fig. 1, the best rotation frequency is determined by Eq. (1); the rated frequency of the turbine will coincide with one of those synchronous frequencies which are nearest the ideal one, adopting the higher or lower value, depending on which of the above considerations may prevail.

The final value of n_s will then be calculated applying Eq. (1) again.

Notations

- D_3 = runner discharge diameter (m)
- g = gravity acceleration (m/s²)
- h_b = barometric pressure (m)
- h_s = static suction head referred to the wicket gate centreline (m)
- h_v = vapour pressure head (m)
- H_n = turbine net design head (m)
- k_u = runner peripheral velocity coefficient
- k_v = ratio between water velocity at spiral case inlet section and spouting velocity
- k_{v1} = ratio between water velocity at draft tube inlet section and spouting velocity
- n = turbine speed of rotation (rev/min)
- n_f = turbine runaway speed of rotation (rev/min)
- n_s = turbine specific speed
- P_t = turbine design capacity (kW)
- Q_o = turbine rated flow (m³/s)
- $Q\gamma$ = flow passing through a spiral case radial section rotated of the angle γ in respect to the inlet section (m³/s)
- r = statistical curves correlation coefficient
- r_1 = distance of a point in the spiral case from the turbine axis (m)
- s = statistical curves standard deviation
- v = water velocity at spiral case inlet section (m/s)
- v_1 = water velocity at draft tube inlet section (m/s)
- v_u = peripheral velocity of water in the spiral case
- σ = cavitation coefficient (Thoma's coefficient)

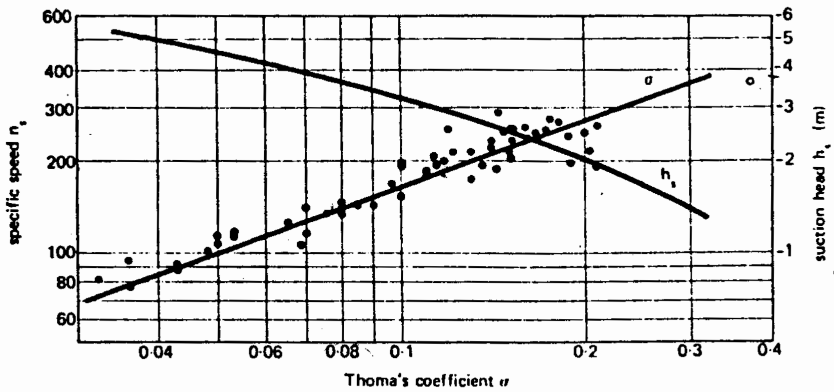

Fig. 3. Cavitation (Thoma's) coefficient and suction head versus specific speed. The rate of change of suction head against specific speed is shown for the period 1970 to 1975, and is seen to vary between —1 to —5m in the range considered.

Strictly related to the value of n_s is the cavitation coefficient, expressed by the formula:

$$\sigma = (h_b - h_w - h_s)/H_n$$

The relationship above expresses the following requirement: to keep the cavitation phenomena within acceptable limits at the turbine discharge, the absolute pressure must not fall below a given value determined by experiment. This depends, in turn, on the elevation above sea level and on the height of the runner above the discharge level. The function

$$\sigma = F[n_s]$$

is shown in Fig. 3.

The available data have led to the following regression curve:

$$\sigma = 7{\cdot}54 \times 10^{-5} n_s^{1{\cdot}41}$$

with

$r = 0{\cdot}95$ $s = 0{\cdot}027$

For every turbine, choosing the value of n_s and σ in Figs. 1 and 3 determines both the maximum value of the suction head h_s and the consequent elevation of the unit in respect to the minimum water discharge level. Furthermore, Fig. 3 gives the rate of change of h_s versus the specific speed obtained on the base of the curve $n_s = n_s(H_n)$ relative to the period 1970–1975, and of the curve $\sigma = F[n_s]$ on the same diagram.

As can be seen, the average suction head h_s varies between -1m and -5m in the range considered. In Fig. 4, the calculated curve is compared with similar curves covering different periods of time. It shows a progressive reduction over the years of the cavitation coefficient for a given specific speed, especially for units where this is high. This illustrates the improvement obtained in the operation of turbines as a result of a more accurate study of their hydrodynamic profiles. The ratio of the runaway rotation frequency n_f to the rated one n, necessary to define the design of the electric generator, is expressed as a function of n_s in Fig. 5. For each turbine the maximum frequency of rotation, relative to the rated opening corresponds to the maximum operating head.

The available data show marked scattering because the ratio between the maximum and the rated head of the unit varies depending on the powerplant.

To give evaluation criteria which as far as possible are independent from these characteristics, the interpolating function has been determined by considering only data pertaining to powerplants for which the maximum head does not differ by more than ten per cent from the rated one. The interpolating function is:

$$n_f/n = 1{\cdot}52 + 1{\cdot}52 \times 10^{-3} n_s$$

where

$r = 0{\cdot}64$ $s = 0{\cdot}12$

For powerplants with considerable head variations, a first approximation value for n_f can be obtained by increasing the value given by the interpolating curve proportionally to the square root of the ratio between maximum and rated heads.

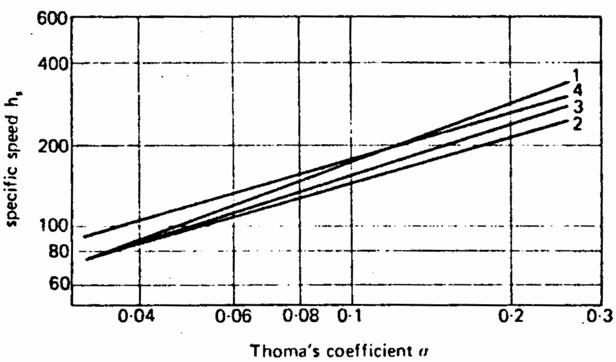

Fig. 4. Cavitation (Thoma's) coefficient decrease as a function of the period of design. The curve denoted by (1) is derived from Fig. 3; curves 2 and 3 are derived from the same sources as curves 2 and 3 in Fig. 2; curve 4 is derived from Turbines hydrauliques et leur regulation *published in 1966 and written by L. Vivier.*

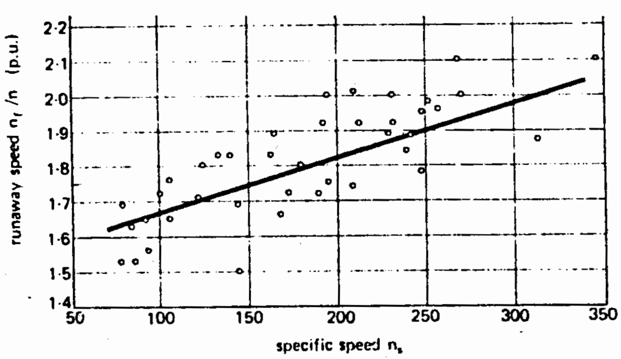

Fig. 5. Ratio between runaway and rated speed versus specific speed. The design of the associated generator depends on the rated speed n.

Runner size

The similarity laws applied to hydraulic turbines show that with the same specific speed, the peripheral velocity coefficient k_u remains constant; k_u is defined by the expression:

$$k_u = D_3 n / [60\sqrt{(2gH_n)}]$$

where: D_3 = discharge diameter of runner; and g = gravity acceleration.

Once the rate of change of k_u versus n_s and the rotation frequency n are established, it is possible to calculate the

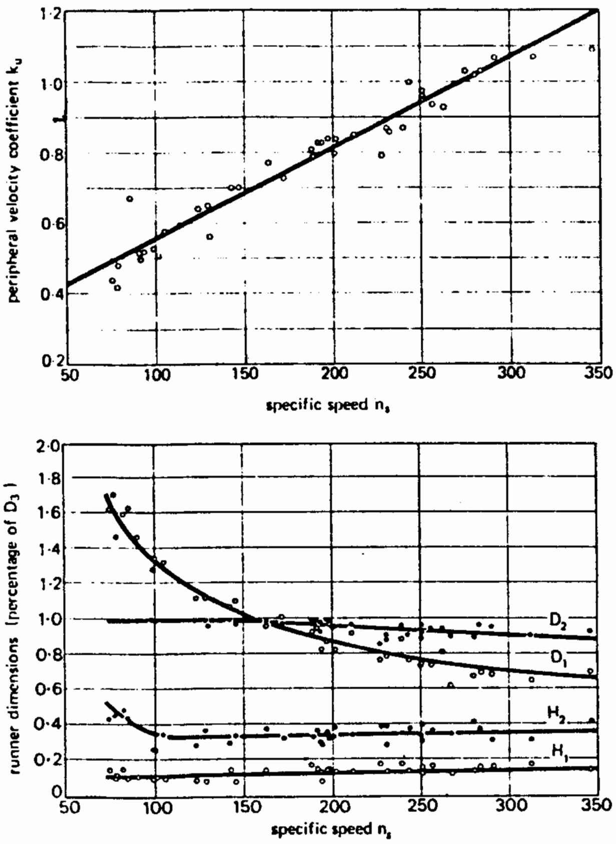

Fig. 6 (top). Peripheral velocity coefficient versus specific speed, and (bottom) main runner dimensions versus specific speed.

value of the discharge diameter:

$$D_3 = 84{\cdot}5k_u\sqrt{(H_n)}/n$$

Fig. 6 (top) shows the data used, and gives the resulting interpolating function:

$$k_u = 0{\cdot}31 + 2{\cdot}5 \times 10^{-3}n_s$$

where

$$r = 0{\cdot}97 \qquad s = 0{\cdot}047$$

The other runner dimensions indicated in Fig. 7 may be obtained in function of n_s, referred to the diameter D_3, from the curves of Fig. 6 (bottom).

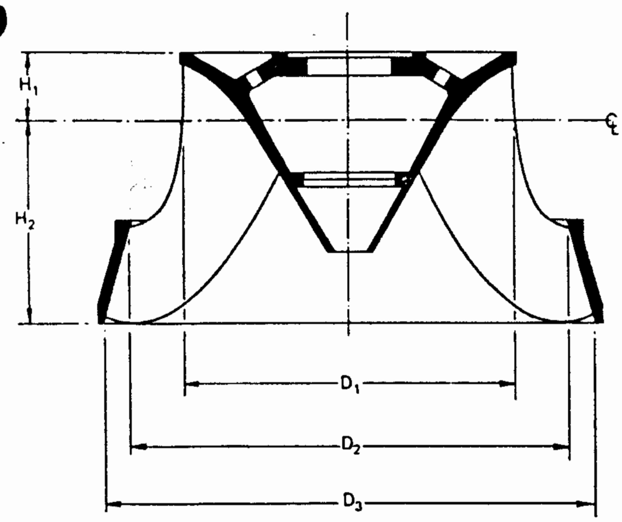

Fig. 7. Runner dimensions; these are dependent on the parameters indicated in the lower diagram of Fig. 6.

The interpolating functions of the various curves are as follows:

$$D_1/D_3 = 0{\cdot}4 + 94{\cdot}5/n_s$$
$$r = 0{\cdot}977 \qquad s = 0{\cdot}075$$

$$D_2/D_3 = 1/(0{\cdot}96 + 0{\cdot}00038n_s)$$
$$r = 0{\cdot}67 \qquad s = 0{\cdot}028$$

$$H_1/D_3 = 0{\cdot}094 + 0{\cdot}00025n_s$$
$$r = 0{\cdot}63 \qquad s = 0{\cdot}023$$

$$H_2/D_3 = -0{\cdot}05 + 42/n_s \qquad (50 < n_s < 110)$$
$$r = 0{\cdot}62 \qquad s = 0{\cdot}056$$

$$H_2/D_3 = 1/(3{\cdot}16 - 0{\cdot}0013n_s) \qquad (110 < n_s < 350)$$
$$r = -0{\cdot}21 \qquad s = 0{\cdot}059$$

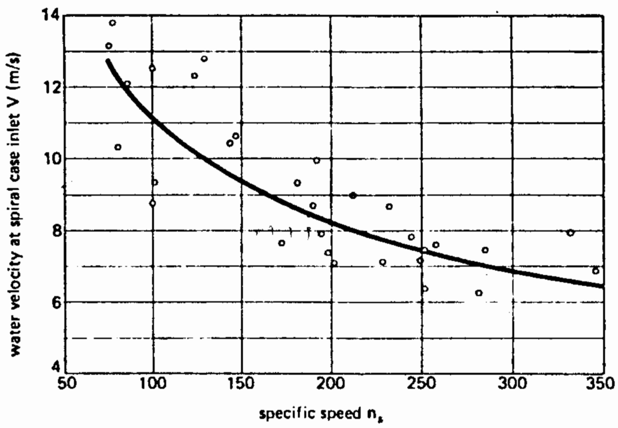

Fig. 8. Water velocity at the spiral case inlet, versus specific speed.

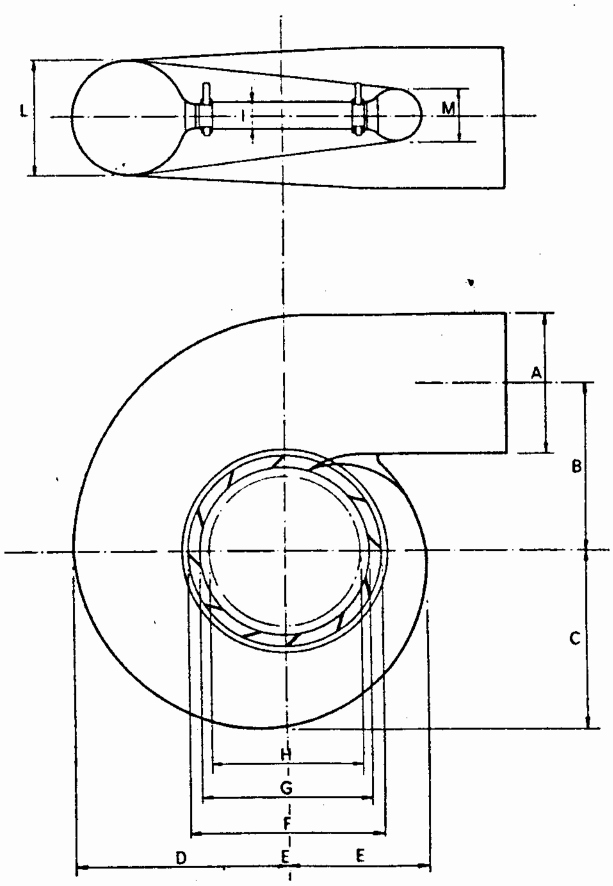

Fig. 9. Main spiral case dimensions; these are dependent on the parameters indicated in Figs. 10 and 11.

The r and s values obtained indicate that, as far as the runner size is concerned, the design criteria of the different manufacturers are very similar.

Spiral casing size

The dimensions of the spiral case depend essentially on the value assumed for the water velocity at the inlet section. Given this value, the areas of the transverse sections are generally calculated as a function of their position along the axis of the spiral casing, so that the following conditions are satisfied:

$$Q\gamma = Q_o(1-\gamma/2\pi) \qquad \ldots \qquad (2)$$

$$v_u r_1 = k \qquad \ldots \qquad (3)$$

Eq. (2) shows that the runner is fed uniformly along its inlet circumference, while Eq. (3) reflects the irrotationality of the water flow.

Fig. 8 gives, as a function of n_s, the average statistical value of the absolute water velocity at the inlet section of the spiral casing, relative to the design head H_n. The interpolating function is:

$$v = 844 n_s^{-0{\cdot}44}$$

$v = -0{\cdot}84 \qquad s = 1{\cdot}267$

The main dimensions of the spiral casing indicated in Fig. 9 may be obtained as a function of n_s, referred to the diameter D_3, from the curves of Figs. 10 and 11. The interpolating functions for the different curves are as follows:

$A/D_3 = 1{\cdot}2 - 19{\cdot}56/n_s$
$r = 0{\cdot}54 \qquad s = 0{\cdot}099$

$B/D_3 = 1{\cdot}1 + 54{\cdot}8/n_s$
$r = 0{\cdot}92 \qquad s = 0{\cdot}082$

$C/D_3 = 1{\cdot}32 + 49{\cdot}25/n_s$
$r = 0{\cdot}84 \qquad s = 0{\cdot}12$

$D/D_3 = 1{\cdot}50 + 48{\cdot}8/n_s$
$r = 0{\cdot}90 \qquad s = 0{\cdot}08$

$E/D_3 = 0{\cdot}98 + 63{\cdot}60/n_s$
$r = 0{\cdot}93 \qquad s = 0{\cdot}08$

$F/D_3 = 1 + 131{\cdot}4/n_s$
$r = 0{\cdot}94 \qquad s = 0{\cdot}15$

$G/D_3 = 0{\cdot}89 + 96{\cdot}5/n_s$
$r = 0{\cdot}94 \qquad s = 0{\cdot}11$

$H/D_3 = 0{\cdot}79 + 81{\cdot}75/n_s$
$r = 0{\cdot}95 \qquad s = 0{\cdot}12$

$I/D_3 = 0{\cdot}1 + 0{\cdot}00065 n_s$
$r = 0{\cdot}87 \qquad s = 0{\cdot}029$

$L/D_3 = 0{\cdot}88 + 0{\cdot}00049 n_s$
$r = 0{\cdot}54 \qquad s = 0{\cdot}06$

$M/D_3 = 0{\cdot}60 + 0{\cdot}000015 n_s$
$r = 0{\cdot}020 \qquad s = 0{\cdot}053$

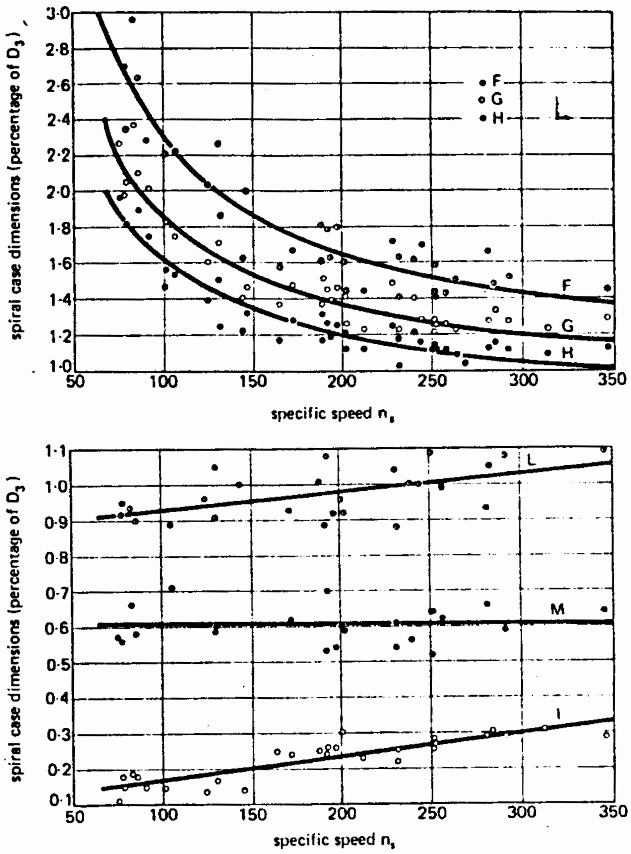

Fig. 11 (top and bottom). Main spiral case dimensions versus specific speed; the letters F, G, H, L, M and I refer to the sizes shown in Fig. 9.

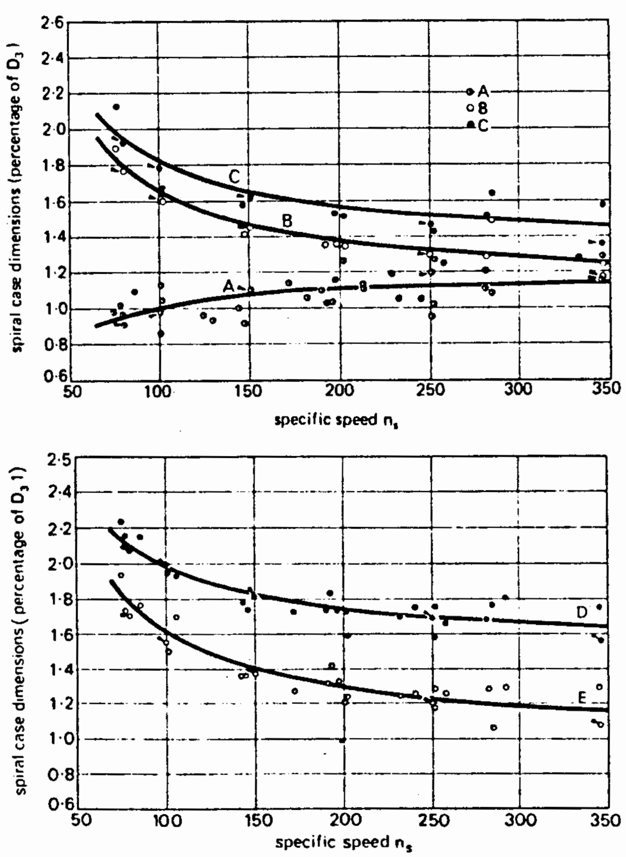

Fig. 10 (top and bottom). Main spiral case dimensions versus specific speed. The points indicated with an arrow refer to spiral cases calculated as controls assuming an average inlet velocity given in Fig. 8. The letters A, B, C, D and E refer to the dimensions indicated in Fig. 9.

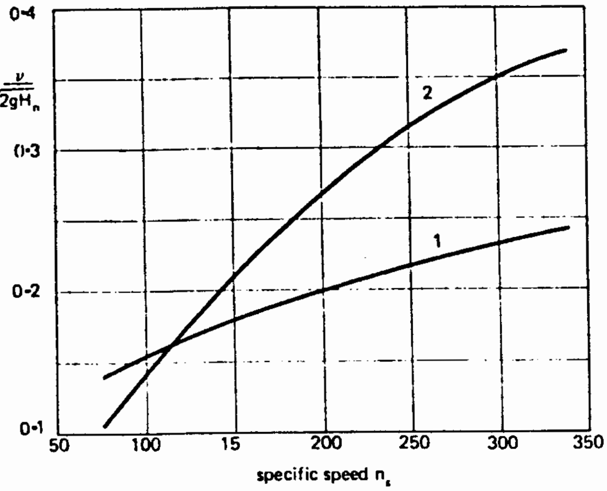

Fig. 12. Ratio between actual and spouting water velocity in (1) the spiral case inlet and (2) the draft tube inlet.

The points marked with an arrow on the diagrams of Fig. 10 refer to spiral casings, calculated as a control in accordance with the criteria expounded above, and assuming the average inlet velocity to be that given by Fig. 8.

The interpolating curves agree with the calculated values; the scattering of the points concerning the utilized data results from the inlet velocity chosen.

Figs. 10 and 11 can be interpreted with the aid of curve 1 in Fig. 12; this relates the rate of change of k_v versus n_s, k_v being the ratio between the velocity v of the water at the inlet section of the spiral case, and the spouting velocity corresponding to the rated head obtained according to Figs. 1 and 8. It may be observed that k_v increases with the increase of n_s, although the velocity v diminishes appreciably. This is because of a technical-economical compromise between two opposing trends, which are:

(*a*) to keep k_v constant and with it the incidence of head losses compared with total head as n_s increases; this would require a major reduction of v which would mean greater dimensions and costs for the spiral casing; and

(*b*) to keep the velocity v constant with the aim of limiting the dimensions of the spiral casing; with all other conditions constant this involves a considerable increase of k_v and therefore an appreciable reduction of the turbine efficiency.

The compromise solution indicated by the statistical curves in Figs. 10 and 11 partially satisfies both requirements, accepting a small reduction in efficiency while still ensuring an economical size for the spiral case.

Accordingly, the diameters A and L increase with the increase of n_s; the apparent anomaly that M remains constant is because of its proximity to the end section of the spiral casing where the volute departs from the theoretical circular shape. The dimensions B, C, D and E of the horizontal sections of the spiral case diminish with the increase of specific speed, in spite of the greater volute diameter. This occurs because, with the increase of specific speed, the inlet diameter of the runner, and consequently the ones of the guide and stay vanes, diminishes compared with the discharge diameter, so that the volute has to be formed around a smaller circumference.

Draft tube size

The draft tube size is directly determined by the size of runner, as both have in common the diameter D_3 and the absolute velocity at the inlet section which corresponds with the runner discharge velocity.

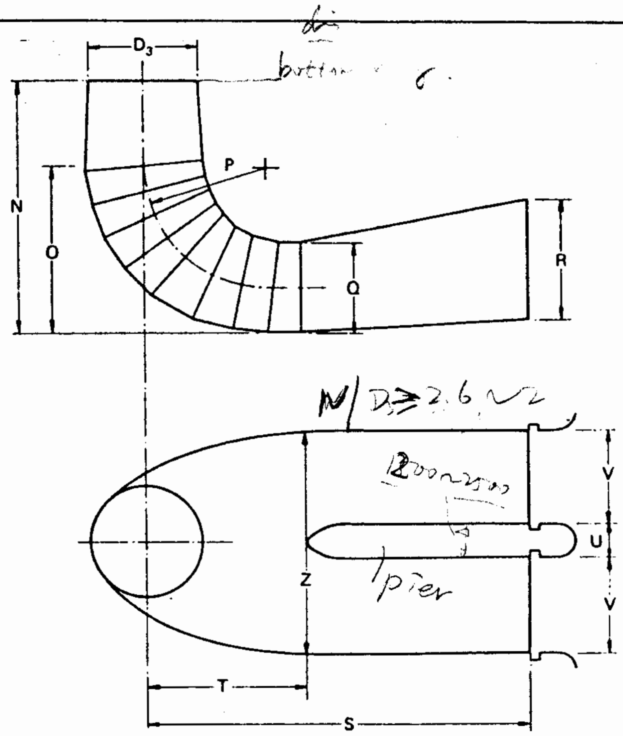

Fig. 13. Main draft tube dimensions. These are determined principally by the relationships indicated in Figs. 14 and 15.

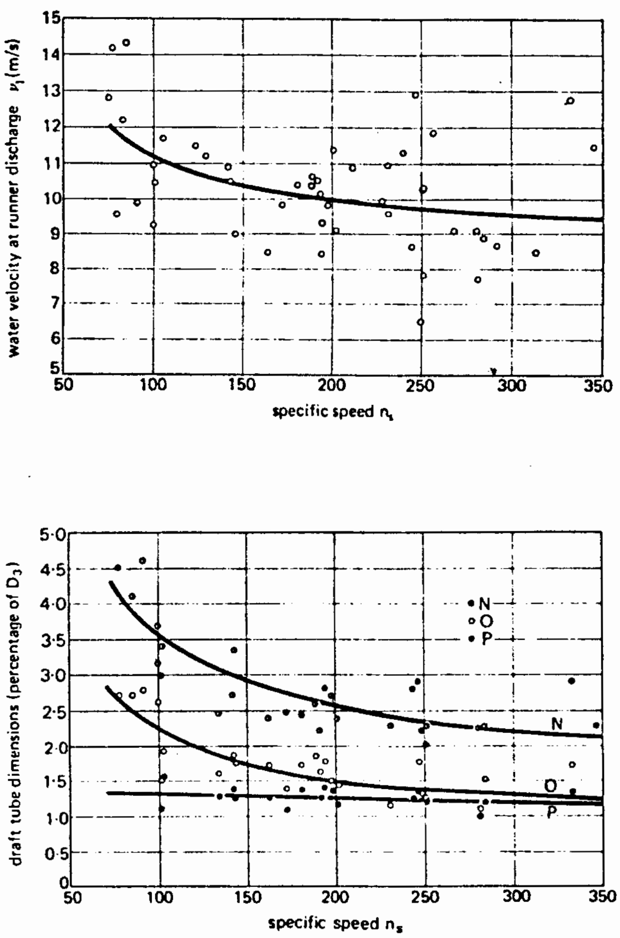

Fig. 14 (top). Water velocity at the runner discharge versus specific speed and (bottom) main draft tube dimensions versus specific speed. The letters N, O and P in the lower diagram refer to specific dimensions shown in Fig. 13.

Fig. 14 (top) gives the mean statistical value of this velocity versus the specific speed n_s. The interpolating function is

$$v_1 = 8{\cdot}74 + 248/n_s$$

where

$$r = 0{\cdot}46 \qquad s = 1{\cdot}45$$

The most important dimensions of the draft tubes indicated in Fig. 13 are given by Figs. 14 and 15, where the interpolating functions are:

$$N/D_3 = 1{\cdot}54 + 203{\cdot}5/n_s$$
$$r = 0{\cdot}85 \qquad s = 0{\cdot}38$$

$$O/D_3 = 0{\cdot}83 + 140{\cdot}7/n_s$$
$$r = 0{\cdot}82 \qquad s = 0{\cdot}28$$

$$P/D_3 = 1{\cdot}37 - 0{\cdot}00056 n_s$$
$$r = -0{\cdot}27 \qquad s = 0{\cdot}13$$

$$Q/D_3 = 0{\cdot}58 + 22{\cdot}6/n_s$$
$$r = 0{\cdot}38 \qquad s = 0{\cdot}15$$

$$R/D_3 = 1{\cdot}6 - 0{\cdot}0013/n_s$$
$$r = -0{\cdot}33 \qquad s = 0{\cdot}25$$

$$S/D_3 = n_s/(-9{\cdot}28 + 0{\cdot}25 n_s)$$
$$r = 0{\cdot}64 \qquad s = 0{\cdot}88$$

$$T/D_3 = 1{\cdot}50 + 0{\cdot}00019 n_s$$
$$r = 0{\cdot}06 \qquad s = 0{\cdot}22$$

$$U/D_3 = 0{\cdot}51 - 0{\cdot}0007 n_s$$
$$r = -0{\cdot}47 \qquad s = 0{\cdot}10$$

$$V/D_3 = 1{\cdot}10 + 53{\cdot}7/n_s$$
$$r = 0{\cdot}61 \qquad s = 0{\cdot}19$$

$$Z/D_3 = 2{\cdot}63 + 33{\cdot}8/n_s$$
$$r = 0{\cdot}21 \qquad s = 0{\cdot}32$$

The figures show that, for increasing values of n_s, the draft tube dimensions and particularly its developed length, related to the S and N values, decrease.

On the other hand, for increasing values of specific speed the ratio k_{v1} between the inlet velocity of the draft tube and the spouting velocity relative to the rated head, increases as shown from curve 2 of Fig. 12, which is obtained according to the statistical curves mentioned previously.

These two facts are in conflict; for a larger k_{v1}, and therefore a greater amount of kinetic energy in the draft tube in relation to the potential energy available, the importance of its recovery increases and this would mean enlarging its dimensions. This is another case of technical-economical compromise between the need to increase the draft tube efficiency and to limit its dimensions and the consequent costs of the civil-engineering work involved. With the high specific speeds that accompany the lower heads, the second concept prevails, because of the large dimensions of the runner, even for units of small capacity.

Conclusions

The design of Francis turbines seems to be characterized by two important factors: on one hand there is a remarkable uniformity of design criteria adopted by different manufacturers all over the world, as shown by the limited scattering of the examined data, especially for the runner design; on the other hand great importance is attached to the economic considerations, ie, the trend to reduce the size of the units, both by increasing the specific speed and by limiting the overall dimensions of the largest compo-

Francis turbines at major hydro schemes

Powerplant	Manufacturer	Year of design	Head (m)	Capacity (MW)	Rotation frequency (rev/min)
Akosombo	Hitachi	1964	69	158	115·4
Albi	Riva Calzoni	1972	347·9	36·62	750
Alcantara	Neyrpic	1965	97	242·6	115·4
Altstafel	Escher Wyss	1963	403	10·3	1500
Ana-Sira	Kvaerner Brug	1968	46	50	150
Angostura	Escher Wyss	1974	100·2	214	128·6
Aswan	LMW	1966	62	180	100
Azumi	Mitsubishi	1969	135·7	110·7	200
Balimela	LMW	1967	257	62	375
Bastusel	KMW	1969	67·6	112·5	136·4
Big Bend	Dominion	1964	117·6	183·8	—
Boundary	Nohab	1966	76·2	155·17	120
Bratsk	LMW	1960	96	217	125
Brommat II	Neyrpic[2]	1969	255	239·7	250
Cabora Bassa	Neyrpic[1]	1969	127	485	107
Caroni Macagua I	Voith	1958	45	72·8	—
Carters	Newport News	1965	106	128	163·6
Cethana	Voith	1967	98·8	101·6	200
Churchill Falls	Neyrpic[5]	1972	312	478	200
Clear Creek	Hitachi	1962	162·6	68·7	225
Corfino	Ansaldo	1968	180·7	15·34	600
Dubrovnik	Neyrpic	1961	290	113·9	300
Dworshak, Wash.	Allis Chalmers	1968	139	254·4	128·6
Edward Hyatt	Allis Chalmers	1963	187·4	118·3	200
El Chocon	Boving	1971	58·4	204·4	88·3
Hendrik Verwoerd	Voith	1972	68·6	102	136·4
Estreito V-VI	Voith	1970	63·3	178·6	112·5
Fadalto	Riva Calzoni	1967	107·32	119·9	176·5
Farahnaz Pahlavi	Riva Calzoni	1965	80	28·87	250
Funil	Ansaldo	1963	71·5	73·6	163
Furnas	Nohab	1963	94	154·4	150
Glen Canyon	Baldwin	1960	138	115	150
Gokçekaya	Allis Chalmers	1967	112	103	187·5
Grançarevo	Riva Calzoni	1961	103·5	61·7	214·3
Grand Coulee III	Dominion[7]	1973	86·8	603	—
Grand Coulee IV	Allis Chalmers	1973	87	700	85·7
Grimsel II	Escher Wyss	1974	458	106	750
Guri	Hitachi	1966	115	218·5	128·6
Harspranget V	KMW	1974	103	469	107·1
Hermillon	Neyrpic	1971	163	61·39	333
Ilha Solteira	Riva-Tosi-Ansaldo[8]	1968	48	194	85·7
Infernillo	Neyrpic	1961	110	205	163·8
Inga I	Tosi-Ansaldo	1968	53·5	66·2	136·3
Inga II	Escher Wyss	1972	62·5	178	107·1
Jaguara	Mitsubishi	1969	48	118	100
Jordan River	Voith	1968	289·5	183	257
Kafue Gorge	Kvaerner Brug	1968	387	154·4	375
Kargamakis	Neyrpic[3]	1970	135	137·8	214
Kesikkopru	Tosi-Ansaldo	1961	41	46·2	125
Kharami II	LMW	1960	307	56·5	428·5
Kossou Bandama	Riva Calzoni	1969	49·5	68·6	125
Krasnoyarsk	LMW	1964	93	508	93·75
Kremasta	Allis Chalmers	1962	112	96·5	166·6
Langenprozelten	Escher Wyss	1972	258·4	30	500
Langsan	KMW	1972	180	52·6	428
La Suassaz	Neyrpic	1970	207	81·6	333
Libby	Allis Chalmers	1970	91·44	121·3	128·6
Loentsch	Escher Wyss	1970	359·2	40·4	750
Lower Tachien	Mitsubishi	1967	295	105·9	360
Magisano	Riva Calzoni	1972	370·3	39·41	750
Malpaso	Escher Wyss	1974	95·5	218·4	128·6
Mangla	Mitsubishi	1967	130·8	147·8	166·7
Manicougan III	Dominion	1976	94·18	197	—
Marimbondo	Neyrpic[4]	1972	72	185	100
Mica	LMW	1975	182·9	444	128·6
Miranda	Vevey	1957	65	58·8	150
Mitta	KMW	1971	203	98·2	333·3
Monte S. Angelo	Tosi-Ansaldo	1966	201·7	84·2	333
Mongiove	Ansaldo	1962	51·6	25	214
Mossy Rock	Nohab	1967	94·5	167·5	128·6
Nakatsugava I	Voith[6]	1969	410	89	500
Niagara Lewiston	Voest[9]	1958	92	150	120
Nurek	KhTBP	1970	230	310	200
Oldan	KMW	1972	252	68·9	500
Outardes III	Dominion	1968	143·5	190	—
Orichella	Tosi	1972	474·4	75·23	600
Paradela	Charmilles	1953	430	55·8	600
Passo Fundo	Mitsubishi	1972	260	112·5	300
Paulo Afonso	Voith	1968	82·5	207	138·5
Pelos	Tosi	1973	124·3	32·85	300
Porjus	KMW	1971	59·5	241·2	83·3
Portage Mountain	Mitsubishi	1967	170·7	266	150
Pradella	Escher Wyss	1964	494	75	750
Reza Shah-Kabir	Neyrpic[3]	1970	165	278	166·7
Rio Acaray	Riva Calzoni	1965	100	47	214·3
Ritsem	KMW	1973	145	330	166·7
Salas	Voith	1970	263	54·7	500
Salto Osorio	Mitsubishi	1972	72	158	120
Sarelli	Escher Wyss	1973	350·2	49	750
Smith Mountain	Voest[9]	1960	55	155	100
Sirikit	Mitsubishi	1972	84·3	150·8	125
Sodusu II	Voith	1973	380	41·2	600
Tagokura	Mitsubishi	1961	118·2	108	167
Tiefencastel II	Escher Wyss	1966	366·6	28·1	750
Tokkeverkene	Kvaerner Brug	1961	209	103	250
Tonstad	Kvaerner Brug	1968	430	165·44	375
Tumut 3	Toshiba	1971	161·5	283	187·5
Ust-Ilim	LMW	1972	90	245	125
Verbano II	Escher Wyss	1970	284	62·8	500
Vessingfoss	Kvaerner Brug	1969	48	38·6	214
Vietas	KMW	1967	67	163	107·1
Vouglans	Vevey	1964	100·2	65	150
Waldeck II	Voith	1970	336·6	220	375
Xavantes	Escher Wyss	1962	73·7	106	128·6
Yarnvagsforsen	KMW	1973	85	54·4	214·3

In cooperation with; 1, Voith; 2, Creusot-Loire and Jeumont-Schneider; 3, SFAC and JS; 4, Creusot-Loire, Voith, Mecanica Pesada and Voith Bresil; 5, Marine Industries; 6, Fuji Denki Seizo K.K. Kawasaki; 7, Willamette Iron and Steel Company; 8, Alsthom, Creusot-Loire, Eschei Wyss, Siemens, and Voith; and 9, BLH.

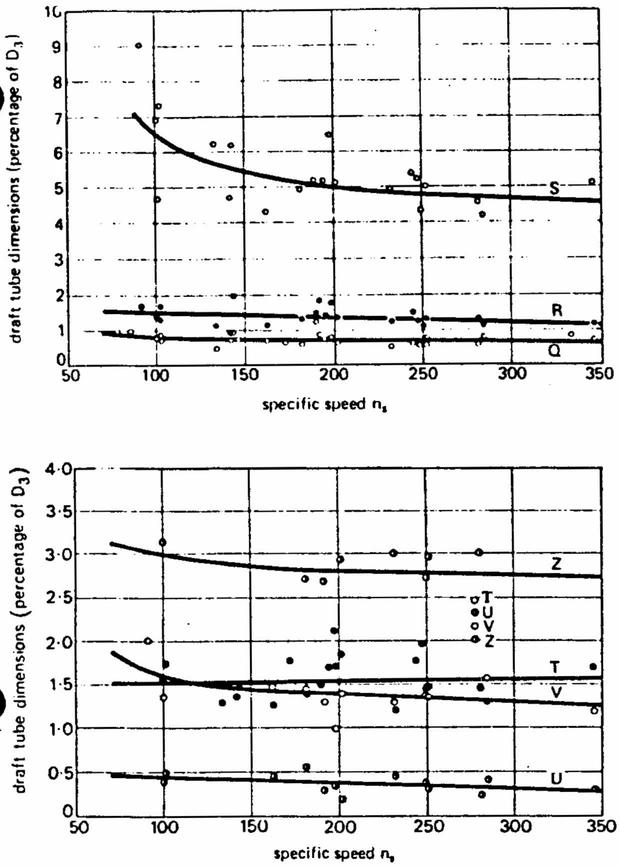

Fig. 15 (top and bottom). Main draft tube dimensions versus specific speed. The letters S, R, Q, T, U, V *and* Z *refer to sizes shown in Fig. 13.*

nents which have the greatest influence on the costs of the civil structures.

This would not be possible without adequate and advanced research programmes, refined and up-to-date technology and improved calculation methods, which allow the operation of the units under more and more severe hydraulic conditions, while at the same time guaranteeing the required reliability. ■

References

1. Baumann, K. M. J. and Podlesak, J. "The Franois turbines of El Infernillo and La Angostura hydroelectric stations in Mexico", *Escher Wyss News*, 1972, No. 1.
2. Shchegolev, S. "Problems in designing and constructing large turbines" *Water Power*, April 1974, p111.
3. Gamous, J. M., Krasilnikov, M. F. and Bryzgalov, V. J. "Operation and design of hydropower equipment for the Krasnoyarsk station" *Water Power & Dam Construction*, January 1975, p21.
4. Siebensohn, R. B. "Trends in U.S. hydro equipment design", *Water Power*, February 1974, p44.
5. "The Aswan high dam", *Water Power*, August 1965, p301.
6. Bohn, M. and Hamon, M. "The Djatiluhur Project", *Water Power*, August 1967, p305.
7. "The Farahnaz Pahlavi project", *Water Power*, August 1968, p305.
8. Barocio, A. J. "Infernillo", *Water Power*, 1965, p198.
9. Rosenstrom, S. "Kafue Gorge hydroelectric power project", *Water Power*, July 1972, p237.
10. Claydon, J. B. "The Peace River project", *Water Power*, September 1965, p339.
11. Lovell, L. A., Lowe, J. and Binger, W. V. "Tarbela dam construction reaches half-way mark", *Water Power*, October 1972, p355.
12. "Kremasta", *Water Power*, April/May 1967, pp133 and 179.
13. Burns, D. R. and Meyers, J. F. "The 700MW Turbines at Grand Coulee Dam", Canadian Electric Association, Spring Session, Montreal, Canada, March 1974.
14. "260 000 PS Francis turbinen für Kraftwerk Estreito, Brazilien", J. M. Voith GmbH, Heidenheim, Germany.
15. "300 000 PS Francis turbinen für Kraftwerk Paulo Afonso, Brazilien", J. M. Voith GmbH, Heidenheim, Germany.
16. "Turbines Hydrauliques", Energomachexport Moscow, USSR, 1971.
17. "Photographs of 93 500 h.p. Francis turbine for Clear Creek Powerplant", Hitachi Limited, Tokyo, Japan.
18. "Furnas power station, Brazil", Nohab, Trollhöttan, Sweden.
19. Kovalev, N. N. "Hydroturbines", Israel Program for Scientific Translations, Jerusalem, Israel, 1965.

A complete reference list is available from the authors.

Design and construction of the Takase river dams

By S. Mimura*

Currently under construction in Japan, this scheme will harness the waters of the Takase river to produce 1280MW. This article deals with the design and construction of the two dams for the project, the Takase and Nanakura, and gives particular emphasis to the materials and their specifications.

THE TOKYO ELECTRIC Power Company, which supplies electricity to an area of 40 000km^2 around Tokyo, is the authority with the largest number of consumers in Japan. During 1974 electric energy supplied by the company reached 105MWh × 10^6 and the maximum output exceeded 21 000MW. The power sources of the company are presently composed of hydropower at 23 per cent, thermal power at 74 per cent and nuclear power at 3 per cent. The long range growth rate of demand for electricity is estimated at several per cent per annum in Japan inspite of the considerable slow growth at present, resulting from the world-wide economic depression, so that the steady increase in installed capacity is still required. To meet peak loads by making the most efficient use of thermal and nuclear plants, it is necessary to construct large-scale pumped-storage powerplants. It is intended to keep the distribution ratio of hydropower at about 20 per cent and the percentages of thermal and nuclear power will change to 60 per cent and 20 per cent, respectively.

*General Manager, Construction Department, The Tokyo Electric Power Company Inc., Uchisaiwai-Cho, Chiyoda-Ku, Tokyo 100, Japan.